SENSORLESS TEMPERATURE ESTIMATION AND CONTROL OF PELTIER DEVICES

by

LAEL ULAM ODHNER

B.S. Mechanical Engineering

Massachusetts Institute of Technology, 2004

Submitted to the Department of Mechanical Engineering
on May 12, 2006 in partial fulfillment of the
requirements for the degree of Master of Science in
Mechanical Engineering
[June 2006]

Signature of Author: .....
Department of Mechanical Engineering
May 12, 2006

Certified By: .....
H. Harry Asada
Ford Professor of Mechanical Engineering
Thesis Supervisor

Accepted By: .....
Lallit Anand
Professor of Mechanical Engineering
Chairman, Department Committee for Graduate Students

SENSORLESS TEMPERATURE ESTIMATION AND CONTROL OF PELTIER DEVICES

by

LAEL ULAM ODHNER

Submitted to the Department of Mechanical Engineering
on May 12, 2006 in partial fulfillment of the
requirements for the degree of Master of Science in
Mechanical Engineering

Abstract

Peltier devices, also known as thermoelectric devices (TEDs), are solid state junctions of two dissimilar materials in which heat transfer and electrical conduction are coupled. A current running through a TED causes heat to flow; likewise, the presence of an external temperature gradient will induce an electrical potential across the TED. The former effect is known as the Peltier effect; the latter is known as the Seebeck effect. While TEDs are used primarily as heat pumps, they can also serve as temperature sensors. This thesis presents the design for a controller which uses a TED to simultaneously sense and control the temperature of a shape memory alloy (SMA) wire. The pulse width-modulating driving circuitry in the controller is capable of measuring the undriven voltage across the TED at a rate of 200 Hz between pulses. A low order ARX model is then used to estimate the SMA temperature. The SMA temperature can be controlled using this estimate. This method will enable the production of large arrays of TED-driven SMA tendon actuators, particularly for large DOF robotic systems.

Thesis Supervisor: H. Harry Asada
Title: Ford Professor of Mechanical Engineering

Table of Contents

1 Introduction

Of the many smart actuator materials currently available, shape memory alloys (SMAs) continue to provide unrivalled energy density due to actuation stresses of over 150 MPa. Because SMA actuators operate by means of a temperature-induced solid-solid phase transition, control performance hinges on the speed and accuracy of heating and cooling the actuator material. The control of SMA temperature is consequently of great interest to the SMA research community.

This thesis focuses in particular on the use of solid-state heat pumps known as thermoelectric devices (TEDs) to heat and cool SMA actuators. In the past, several research groups have explored TEDs as a potential means of driving SMA wires [1]-[3]. Numerous practical benefits arise from the use of TEDs to actuate SMA wires. Most importantly, TEDs are bidirectional heat pumps, so unlike resistive heating, they can cool SMA wires quickly, thereby decreasing actuator response times [1]. Since TEDs are solid state devices, compact and reliable actuator systems can be built, which are not degraded by poor heat transfer rate of air cooling and are free of messy liquid coolants in contact with the SMA wires. Additionally, the external heating provided by TEDs does not depend on the resistance of the SMA wires, unlike Joule heating. However, open loop current driving of TEDs does not provide adequate control over SMA temperature [4]. In order to achieve precision control of an SMA wire via thermoelectric heating and cooling, this paper aims to develop a methodology for measurement and control of the SMA temperature.

The authors were motivated by the need for a controller for a five-fingered robotic hand with SMA actuators driven by TEDs [5]. As shown in Fig. 1, many SMA wires are laid across an array of TEDs, where each SMA axis is connected to a tendon that activates an individual joint of the robotic hand. Twelve axes of SMA actuators are housed in a compact case, which is as thin as a few printed circuit boards. A salient feature of this TED-based SMA drive is that each column of TEDs along a SMA wire allows for local and selective heating and cooling of individual segments of the SMA

wire [5]. The total displacement of a SMA actuator is controlled by varying the number of SMA wire segments which are heated into the Austenitic phase or cooled into the Martensitic phase. Thanks to the bi-stable nature of the SMA phase transition, this segmented binary control is not significantly affected by the hysteresis of the SMA phase transition, and is robust to phase transition disturbances caused by varying tensile loads on the tendon. However, many independent temperature controllers are needed to control the temperature of each tendon actuator. These temperature controllers were previously implemented by placing a thermocouple at each segment, but the complexity of routing sensor wires to each TED and the associated circuitry for reading each thermocouple render this approach inadequate for use with a large array.

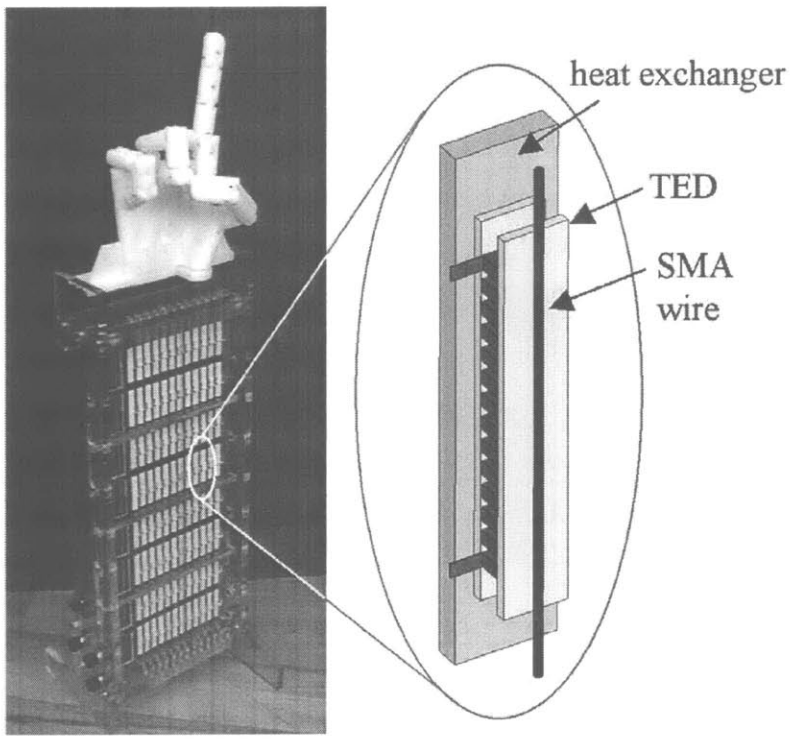

Fig. 1. A robot hand driven by a segmented binary SMA actuator array. A grid of TEDs is used to heat and cool the SMA wire segments. A CAD model of a single TED is shown enlarged. The SMA wires are held in contact with the TEDs using a thermally insulating plate (not shown).

The innovation described in this thesis arises from the fact that TEDs are fundamentally quite similar to thermocouples from a physical perspective. The Peltier effect by which a TED moves heat in response to current is intrinsically linked to the Seebeck effect by which a voltage is generated in response to a temperature difference. Both effects result from the same material property – the relationship between charge carrier mobility and temperature in conducting materials [6]. Because of this, it is possible to use an array of TEDs both as temperature sensors and as heat pumps to control the temperature of each SMA wire segment using only one temperature sensor in the array cooling system for an external reference point.

The new control system utilizes the Seebeck effect to estimate the temperature of the SMA by means of a dynamic model whose structure is physically motivated and whose coefficients are subsequently obtained using least squares system identification. This estimated temperature is then used to control the SMA temperature using proportional feedback control. The design of the TED array and the driving circuitry is presented in section II. Section III presents the derivation of a lumped-parameter dynamic model of a single TED. Experimental verification of the estimation model is shown in section IV, where it is applied to feedback control.

2 Controller and Actuator Design

The target application of this estimation-control technique is a twelve axis tendon actuator for a five-fingered robot hand, as described previously in section I. Each tendon can be controlled to one of eight different displacements, corresponding to eight identical 5 mm by 30 mm TEDs (Purchased from TE Technology, Inc.), spaced 3 mm from each other. The axes are laid out next to each other, forming a grid of TEDs on a water-cooled heat exchanger. The hand and a CAD model of single segment are shown in Fig. 1. The TED temperature estimator must be accurate to within 2-3 °C over a temperature range of 50-100 °C. It is desirable to minimize the response time of the actuator, so the estimator-controller must respond at least as quickly as it would if controlled with an external temperature sensor.

2.1 Electronic Circuit Design

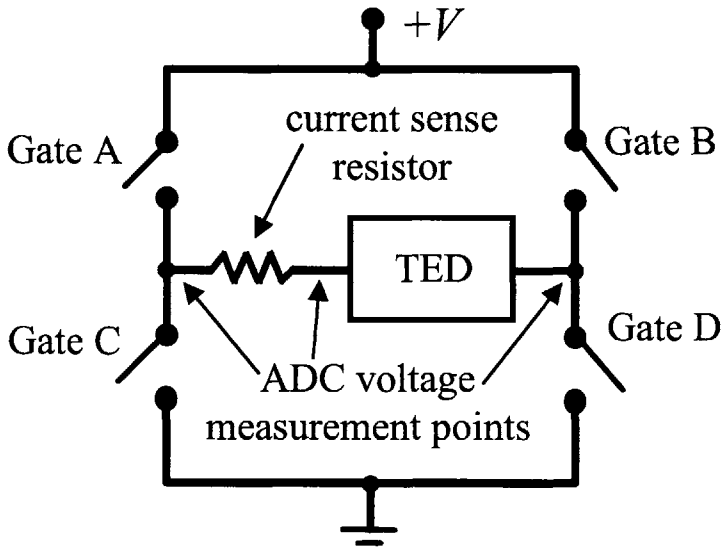

Fig. 2. A schematic showing the H-bridge driver configuration of the TEDs. Gates A and D are closed for heating, gates B and C are closed for cooling. Between current pulses, all gates are left open so that an ADC can be used to measure the Seebeck voltage across the TED. A current sense resistor is placed in series with the TED to measure driving current.

The control system for each TED consists of a specially designed current driver and a sensing circuit. Current is delivered to the TED with an H-bridge amplifier to allow bi-directional driving, as shown in Fig. 2. The amplitude of the driving current is varied by varying the pulse width of the driving signal. Between pulses, the four transistors on the bridge are turned off, enabling the measurement of the unconstrained voltage at both terminals of the TED. Analog to digital converters sample the floating voltages at either side of the TED. These measurements are then subtracted to obtain the Seebeck voltage. While the TED is driven, the voltage across a current sense resistor in series with the TED is sampled to measure the driving current.

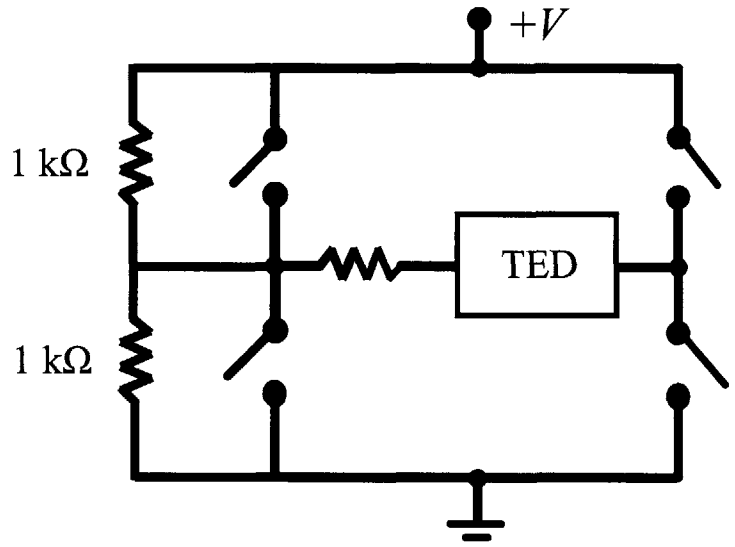

Fig. 3: Saturation due to improperly constrained voltages can be fixed using a high impedance voltage divider connected to one of the two terminals of the TED.

One problem encountered during the development of the Seebeck voltage measurement circuit bears mention here. While the relative voltage between the two sides of the TED converged quickly and consistently to the Seebeck voltage, slightly uneven current leakages in the H bridge transistors were sometimes observed to pull the floating voltage at one terminal close to the power or ground voltage. In this case, the analog-to-digital converters can be saturated, providing artificially low measurements of the Seebeck voltage. To correct this, all that is needed is a pair of 1000 ohm resistors at one

terminal of the TED, one attached to power and the other to ground. These resistors act as a voltage divider, drawing little power but enough that the uneven current leakage does not cause the Seebeck voltage measurement to saturate.

Figure 4 shows a plot of the voltage across a TED resulting from this driving scheme. The plot illustrates the process of switching back and forth between the sensor and heat pump modalities. Due to the low inductance and electrical capacitance of thermoelectric devices, the Seebeck voltage obtained with this sampling circuit is available at relatively high time resolution. A driving/sampling rate of 200 Hertz was selected for the finished controller.

The sensing and driving capabilities of the controller are combined in a central processing unit, which uses the Seebeck voltage to estimate the SMA temperature T_{SMA}. This estimate is used to compute a proportional feedback signal, which is saturated and converted into a pulse width for the driver, as shown in Fig. 5. The control system runs on a Microchip dsPIC30F2010 microprocessor clocked at 8 megahertz. The estimator was implemented as an auto-regressive/exogenous (ARX) input model downsampled from 200 HZ to 50 Hz for estimation and control. The pulse width modulation was handled using the dsPIC30F2010's built-in pulse width modulation module. The computation required for control proved simple enough that multiple axes can be run off of a single controller; the test apparatus was capable of performing all of the temperature estimation and control calculations for two TEDs within 1 millisecond.

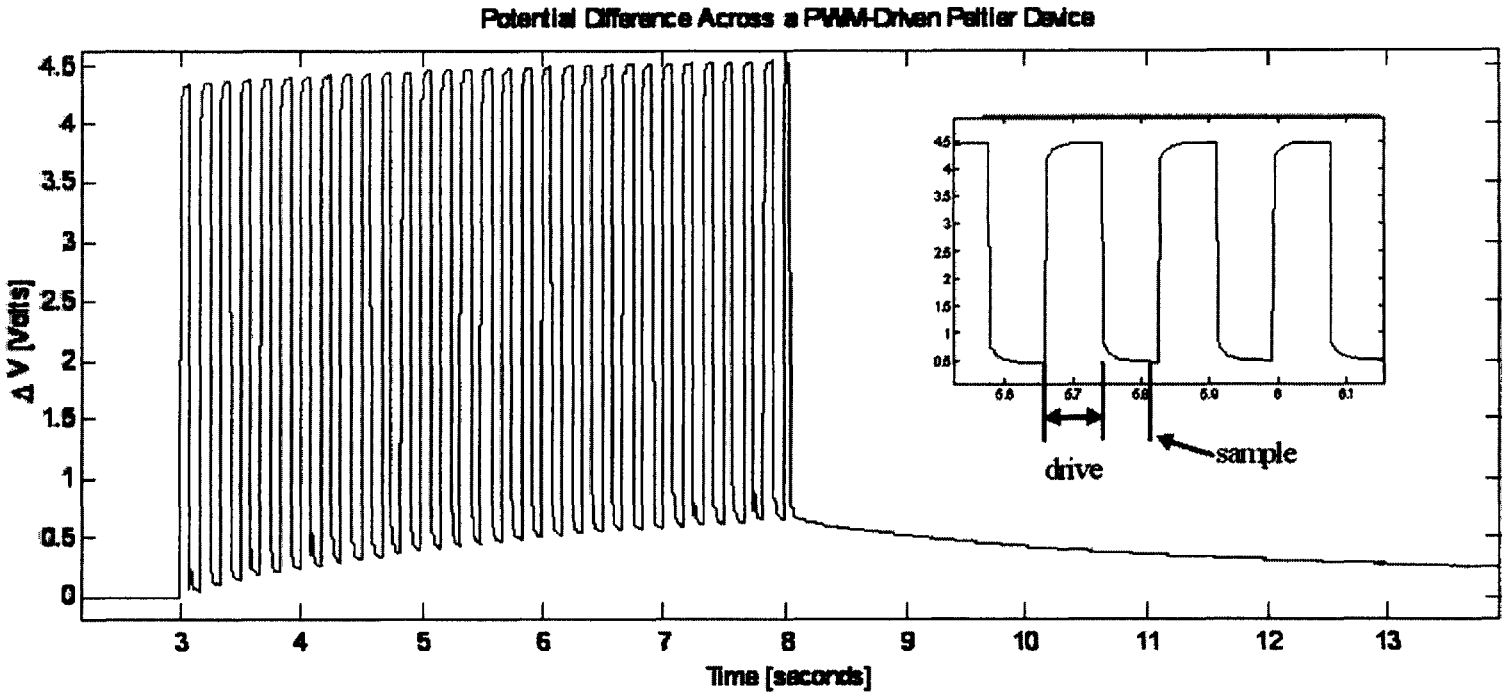

Fig. 4. The voltage difference across a TED is measured while driving at a 50% duty cycle for 5 seconds. The changing Seebeck voltage corresponding to an increase in temperature across the TED can be seen in the rising voltage between pulses. The inset figure shows how the driving and sampling actions were timed.

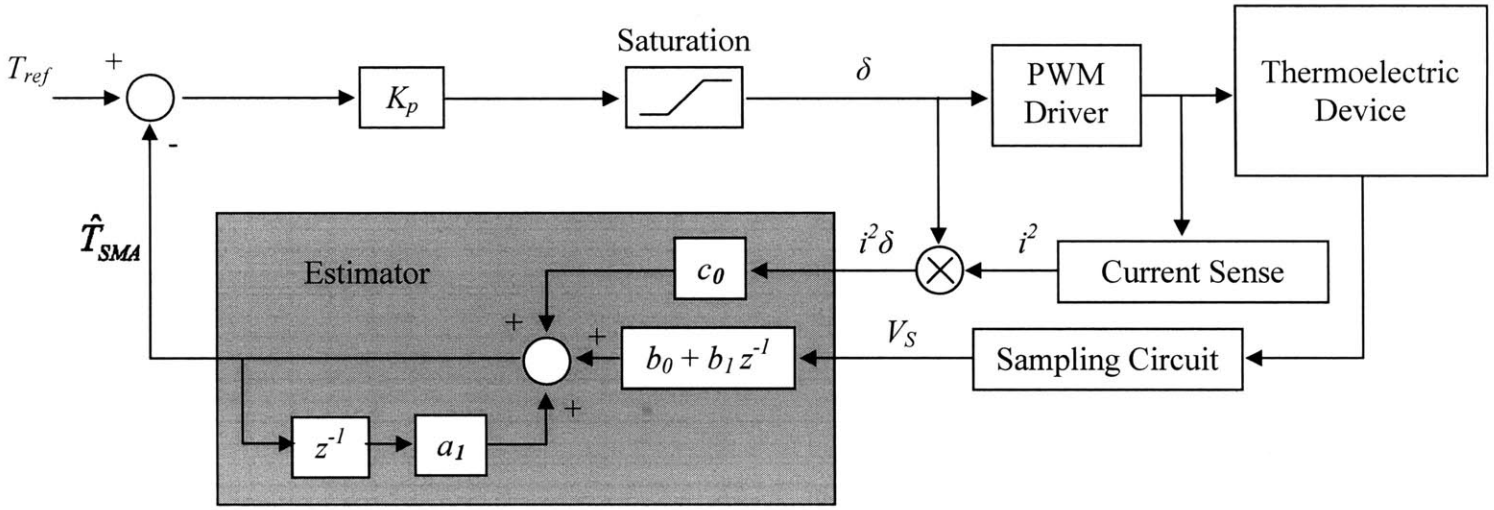

Fig. 5: A block diagram of the control system, including the estimator.

2.2 Thermal System Design

The Seebeck effect measures the local temperature between the SMA wires on one surface of the TED and the heat exchanger on the other surface of the TED. Normally, the reference or "cold" junction is measured with a second thermocouple. In this case, the common reference point for all of the TEDs is the temperature of the heat exchanger, as shown in Fig. 6. To ensure that the temperature on this heat sink was uniform, the heat exchanger was made from a brass sheet several millimeters thick. The high internal conductivity of the brass sheet ensures the uniformity of the heat exchanger temperature, so that a single temperature measurement is a good predictor of the surface temperature everywhere on the heat exchanger.

The heat exchanger temperature was measured using a single thermocouple (Omega 0.25 mm diameter J-type) fastened onto the manifold using conductive heat sink compound. Coolant water is circulated inside the heat exchanger, carrying away waste heat rapidly enough that the heat exchanger temperature T_C could be treated as quasi-stationary. The SMA wire was held against the other surface of the TED with a foamed polystyrene sheet, so that it provides an essentially adiabatic boundary condition for the TED. For calibration and validation, the temperature of the SMA was measured using another 0.25 mm thermocouple. The thermocouple, having the same diameter as the SMA wires used, had contact geometry similar to an SMA wire. Consequently, it provides an adequate measurement of the SMA wire temperature.

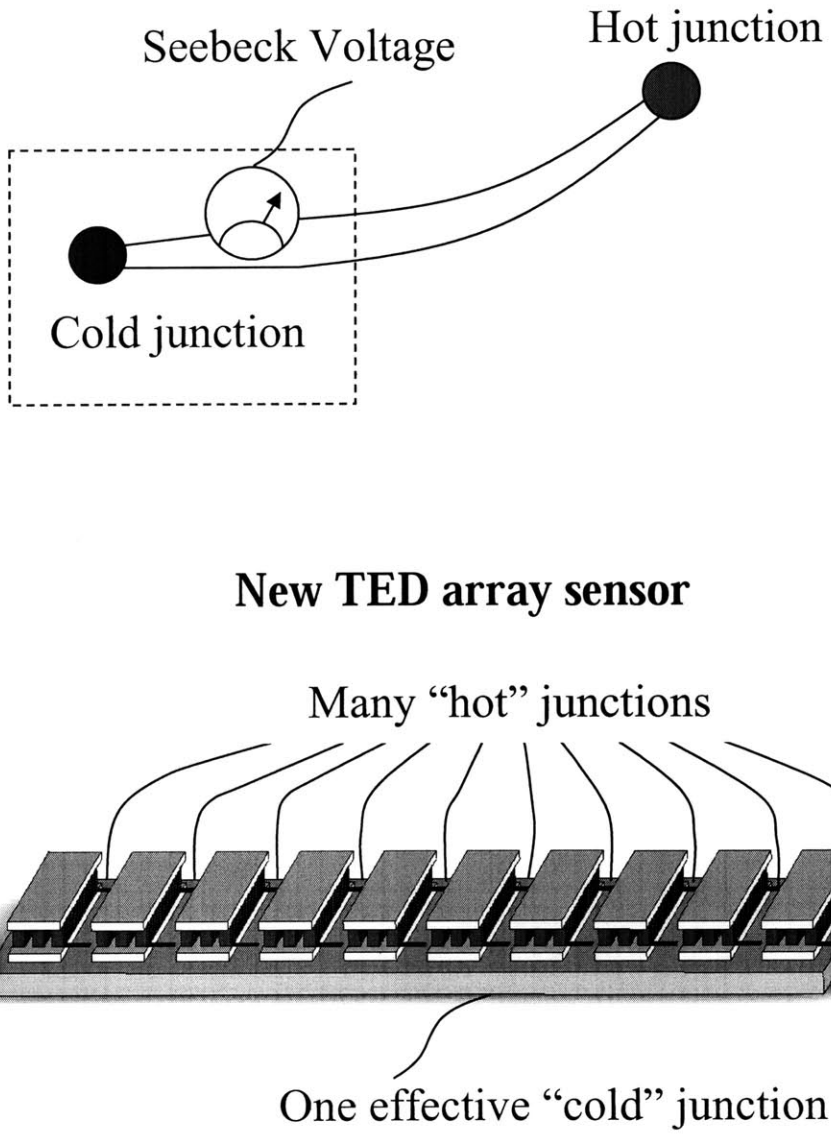

Fig. 6: The array sensor differs from a traditional thermocouple because the reference temperature is provided by the heat exchanger temperature, rather than a second thermocouple at a known temperature.

2.3 Final Hardware Notes

There are multiple aspects of this thermal array hardware that can be modified to suit a particular application while still supporting the estimator-controller models. The water cooling, while quite effective, could be replaced with an air cooling loop, as long as the spatial and temporal stability of the heat exchanger temperature can be guaranteed. The most important aspects of the heat exchange system, upon which the analysis in section III rests, are the boundary conditions at either side of the TED. The surface of the TED in contact with the SMA must not allow heat to flow at steady state. Similarly, the surface of the heat exchanger must be at a uniform temperature, if one sensor is to accurately determine the absolute temperature reference for all of the TEDs. These conditions were deliberately chosen to simplify the modeling and limit the amount of hardware necessary to accurately predict and effectively control the temperature across the whole array.

3 Model Development

In order to estimate the temperature of the SMA using the heat exchanger temperature and the Seebeck voltage, a physical model must be constructed of the thermal behavior of the TED. Two models are presented in this section. The first, a steady-state model resembling a conventional thermocouple measurement, is insufficient for the purpose of control, but nonetheless is instructional and serves as a framework from which a more comprehensive model can be built. The second model accounts for the transient thermal response of the TED, and substantially improves the closed-loop response time of the system.

3.1 Steady-State Model

In all thermoelectric junctions, the Seebeck voltage V_S provides information about the local temperature difference between the two sides of the junction. This relationship is usually described using a lumped Seebeck coefficient β, for a mean material temperature T [6]:

$$\beta(T) = \left(\frac{\partial V_S}{\partial \Delta T} \right)_T \tag{1}$$

In many materials, β varies little over a large enough temperature range that it can be approximated by a constant value. In the TEDs used, β was observed to be constant between 20 °C and 100 °C, so the temperature across the junction ΔT_{TED} was considered to be linearly proportional to V_S,

$$\Delta T_{TED} = \beta^{-1} V_S \tag{2}$$

Using this relationship, the steady-state SMA temperature can be modeled as shown in Fig. 7 as the temperature difference across the TED, ΔT_{TED}, plus the temperature difference between the common reference of the heat exchanger T_C and the temperature at the interface between the TED and the heat exchanger, ΔT_{HE},

$$T_{SMA} = T_C + \Delta T_{HE} + \Delta T_{TED} \tag{3}$$

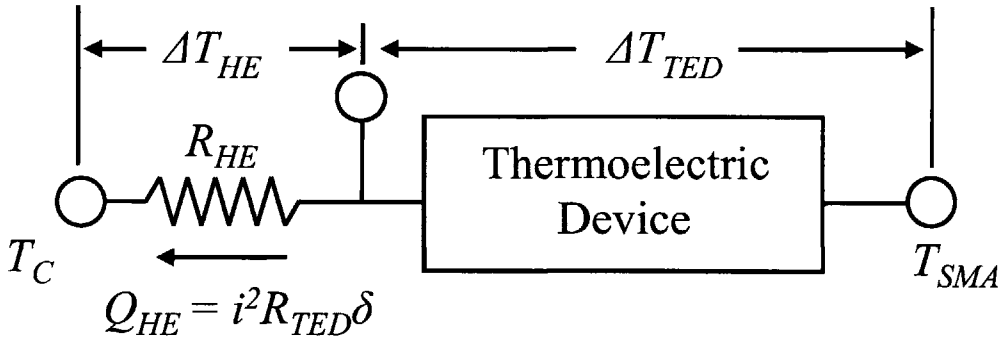

Fig. 7: A static model of the TED. The temperature across the TED ΔT_{TED} is measurable via the Seebeck voltage. The temperature rise due to the thermal interface resistance R_{HE} is found by computing the heat flow Q_{HE}.

When the TED is working as a heat pump, it generates heat due to Joule heating, proportional to the instantaneous driving current i squared and scaled by the duty cycle δ of the pulse width-modulated input,

$$Q_{HE} = i^2 R_{HE} \delta \tag{4}$$

where R_{TED} is the lumped electrical resistance of the TED. The surface of the TED contacting the SMA is assumed to be well enough insulated that no substantial amount of the dissipated heat flows out. Conservation of energy then dictates that the power dissipated within the TED due to Joule heating must be equal to the heat flowing into the

heat exchanger through some interface resistance R_{HE}. This implies that $\Delta T_{HE} = Q_{HE}R_{HE}$. Substituting (4) and (2) into (3) yields

$$T_{SMA} = T_C + d_{ss}P + b_{ss}V_S \tag{5}$$

where

$$P = i^2\delta, \qquad d_{ss} = R_{HE}R_{TED}, \qquad b_{ss} = 1/\beta \tag{6}$$

This parameterization is useful because it makes T_{SMA} a linear function of P and V_S. The parameters b_{ss} and d_{ss} are identifiable from calibration data, and can accurately predict the steady state behavior of the system, but unfortunately (6) is an unfit for estimating a feedback signal. The difficulty with this model is the optimism inherent in the steady state assumption. By controlling the TED based only on the steady-state temperature prediction, the controller cannot observe the transient lag in system response due to thermal capacitance. Consequently, the controller does not exert any effort to cancel the transient lag in response, and tracking performance is poor. To fix this shortcoming, some dynamic model of the TED capacitive behavior is needed.

3.2 Dynamic Model

The transient thermal behavior of a thermoelectric junction is inherently a continuum problem, involving the time-dependent thermal gradients within the TED material. Nonetheless, a simple lumped-parameter pole and zero model of the temperature response is desired for the purpose of control. Some bulk temperature and capacitance simplifications must be made in modeling the TED thermal gradients in order to do this. The capacitive thermal energy of the TED, U_{TED} , can only be expressed as an integral of the thermal capacitance of a thin cross section $c(x)$ and the temperature gradient $T(x,t)$:

$$U_{TED}(t) = \int_0^L c(x)T(x,t)dx \tag{7}$$

In general, it is possible to separate the temperature response of a body of thickness L undergoing transient heat conduction into a series of separable spatial and temporal functions [7]:

$$\frac{T(x,t)-T(0,t)}{T(L,t)-T(0,t)} = \sum_{k=0}^{\infty} \varphi_k(x) f_k(t) \tag{8}$$

Under sufficiently slow input conditions, the higher order terms of this series die away over time, leaving only the lowest order response in the desired separable form. The time constant which governs the decay of the higher-order terms is found by computing the Fourier number, a dimensionless group written in terms of the TED material density ρ, heat capacity c_p, conductivity k, and thickness L:

$$Fo_{0.5L} = \frac{k\,t}{\rho\, c_p\,(0.5L)^2} \tag{9}$$

According to the data published by the manufacturer of the TED, ρ = 7180 kg/m^3, c_p = 179 J/kg K , k = 1.67 W/m K, and L = 1.2 mm [8]. Evaluating the above Fourier number with these data yields $Fo_{0.5L} = t/0.27$ s, from which the characteristic settling time of the temperature gradient is determined to be 0.27 seconds, significantly shorter than the observed system response time of approximately 3 seconds. Because of this, the first-order separable functions $\varphi_0(x)$ and $f_0(t)$ should adequately describe the TED temperature.

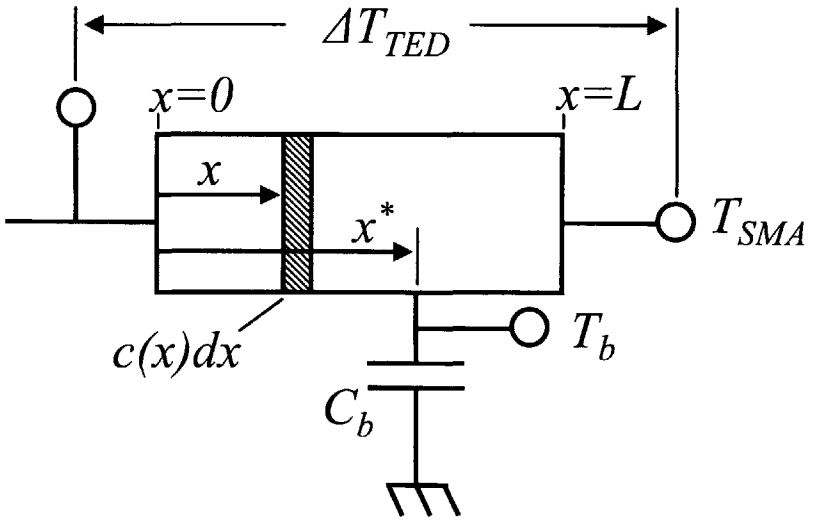

Fig. 8: A dynamic model of the TED. A bulk thermal capacitance assumption was used to describe the lag in transient response due to thermal capacitance. The Seebeck voltage still accurately captures the temperature drop across the TED; However, the heat flow from the TED into the heat exchanger depends on the capacitive effects as well as the Seebeck voltage.

Using this in (8) yields

$$U_{TED}(t) = \int_0^L c(x)\varphi_0(x)f_0(t)dx = f_0(t)\int_0^L c(x)\varphi_0(x)dx \tag{10}$$

According to the mean value theorem, a time-invariant position x^* must exist somewhere within the TED for which the value at x^* is equal to the average value of $c(x)\ \varphi_0(x)$:

$$c(x^*)\varphi_0(x^*) = \frac{1}{L}\int_0^L c(x)\varphi_0(x)dx \tag{11}$$

Using this value of x^*, (7) can be rewritten in terms of a bulk capacitance and a bulk temperature:

$$U_{TED}(t) = L \cdot c(x^*)\varphi_0(x^*)f(t) = L \cdot c(x^*)T(x^*,t) \tag{12}$$

The bulk temperature T_b is defined as $T(x^*, t)$, and the bulk capacitance C_b is defined as $Lc(x^*)$. Figure 5 depicts this augmented parameterization of the TED system. An energy balance can be written for the bulk temperature in terms of Joule heating as a function of the current duty cycle δ and the conductive heat transfer into the heat exchanger:

$$\dot{U}_{TED} = C_b \dot{T}_b(t) = R_{TED} P(t) + \frac{T_C(t) - T(0,t)}{R_{HE}} \tag{13}$$

The temperature $T(0, t)$ at the base of the TED must be directly related to the bulk temperature and the temperature across the TED ΔT_{TED} by means of the same separability argument made in (11):

$$T(0,t) = T_b(t) - \alpha \Delta T_{TED}(t) \tag{14}$$

where α, ranging between zero and one, is a time independent property of the temperature gradient:

$$\alpha = \frac{T_b(t) - T(0,t)}{\Delta T_{TED}} = \frac{\varphi_0(x^*) - \varphi_0(0)}{\varphi_0(L) - \varphi_0(0)} \tag{15}$$

Relating $T(0, t)$ back to T_b and ΔT_{TED} enables the construction of a differential equation and a transfer function dependent only on the dissipative input $P(t)$, the coolant temperature $T_C(t)$ and the TED temperature difference $\Delta T_{TED}(t)$, which can be measured using the Seebeck voltage:

$$R_{HE} C_b \dot{T}_b(t) + T_b(t) = R_{HE} R_{TED} P(t) + T_C(t) + \alpha \Delta T_{TED}(t) \tag{16}$$

$$T_b(s) = \frac{T_C(s)}{R_{HE} C_b s + 1} + \frac{R_{TED} R_{HE} P(s)}{R_{HE} C_b s + 1} + \frac{\alpha \Delta T_{TED}(s)}{R_{HE} C_b s + 1} \tag{17}$$

The SMA temperature T_{SMA} can be related to the bulk temperature T_b in a manner very similar to (14),

$$T_{SMA}(t) = T_b(t) + (1-\alpha)\Delta T_{TED}(t) \tag{18}$$

Equation (18) is then substituted into (17) to obtain a complete transfer function for estimation:

$$T_{SMA}(s) = \frac{T_C(s)}{R_{HE}C_b s + 1} + \frac{R_{TED}R_{HE}P(s)}{R_{HE}C_b s + 1} + \left(\frac{\alpha}{R_{HE}C_b s + 1} + 1 - \alpha \right) \Delta T_{TED}(s) \tag{19}$$

Because (2) allows for the measurement of ΔT_{TED}, (19) is expressible in terms of quantities which can be measured:

$$T_{SMA}(s) = \frac{T_C(s)}{R_{HE}C_b s + 1} + \frac{R_{TED}R_{HE}P(s)}{R_{HE}C_b s + 1} + \frac{(1-\alpha)R_{HE}C_b s + 1}{R_{HE}C_b s + 1} \beta^{-1} V_S(s) \tag{20}$$

From this it can be seen that the SMA temperature is related to the inputs via a common pole, as well as a zero in V_S. For the purpose of computation, (20) was converted to an equivalent ARX model in discrete time. Rather than identifying R_{TED}, R_{HE}, C_b and α directly, the coefficients of the ARX model a_1, b_0, b_1, c_0, and d_0 were treated as a new set of model parameters, which were identified directly using least squares estimation:

$$T_{SMA,t} = a_1 T_{SMA,t-1} + c_0 T_{C,t} + d_0 P_t + b_0 V_{S,t} + b_1 V_{S,t-1} \tag{21}$$

This ARX model bears a striking resemblance to the steady-state model derived in (5). In fact, the coefficients of the two models must be compatible for constant inputs. This is a powerful observation because it greatly simplifies the process of identifying the time-dependent model coefficients. The steady state model, once calibrated, can be used to reduce the number of parameters in the transient which need to be identified, as follows:

$$\frac{c_0}{1-a_1} = 1, \qquad \frac{b_0 + b_1}{1-a_1} = b_{ss}, \qquad \frac{d_0}{1-a_1} = d_{ss} \tag{22}$$

When these constraints are applied to (21), the number of parameters which must be identified in the transient case reduces to two, b_0 and b_1:

$$T_{SMA,t} = T_{SMA,t-1} + b_0\left(\frac{T_{C,t} + d_{ss}P_t - T_{SMA,t-1}}{b_{ss}} + V_{S,t}\right) + b_1\left(\frac{T_{C,t} + d_{ss}P_t - T_{SMA,t-1}}{b_{ss}} + V_{S,t-1}\right) \quad (23)$$

Model order reduction using the steady state model makes parameter identification simpler, but it has another, subtler advantage: Predictions made using this model will have minimal steady-state error, as they are algebraically constrained to the steady-state model. No drift in estimation will occur due to improperly identified system poles, which is crucial to maintain accuracy in temperature control.

4 Experimental Results

An estimator-controller for two SMA segments was implemented using the model of (23). Calibration of the steady-state parameters b_{ss} and d_{ss} was performed by hand, yielding values of 98.4 °C/V for b_{ss} and 7.37 °C/A^2 for d_{ss}. The agreement between the calibrated static model and measured values of T_{SMA} is shown in Fig. 9. The 95.5 percent agreement of the TED behavior with the linear model confirms the validity of the two-term model from (5), and also the assumption that the Seebeck coefficient β is constant up to at least 100 °C.

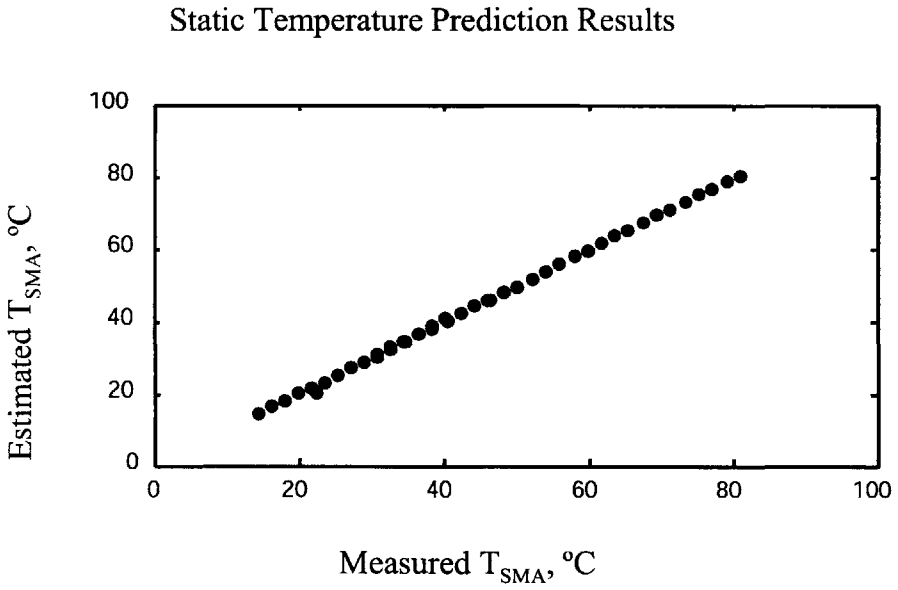

Fig. 9: The static temperature estimator, which predicts T_{SMA} using dissipated heat and Seebeck voltage, is found to agree to within 95.5% with the steady-state temperature measurements.

The dynamic model parameter identification was performed onboard the controller using an automatic calibration routine. In this way, the exact timings used by the microcontroller were reflected in the dynamic model. The dynamic model was compared with the tracking performance of the controller using identical gain and an off-the-shelf thermocouple as an external feedback sensor. A reference trajectory was chosen

typical of the desired behavior SMA actuator array, switching between 70 and 85 °C at 5 second intervals. The response, plotted in Fig. 10, shows that the estimator-controller performs comparably to an external sensor used for feedback. Steady-state average tracking error using a sensor was measured to be –0.9 °C; using the dynamic estimator, the average error was –1.4 °C. A lag following each large change in the reference signal was observed in the response of both the sensored and sensorless controllers. This lag, which limited the maximum rate of tracking response, was caused by the output saturation of the controller.

Figure 10 also includes a response generated by using the static estimator for feedback control. As discussed in III, the steady state behavior of the controller is still accurate, but the settling time is much longer than desirable.

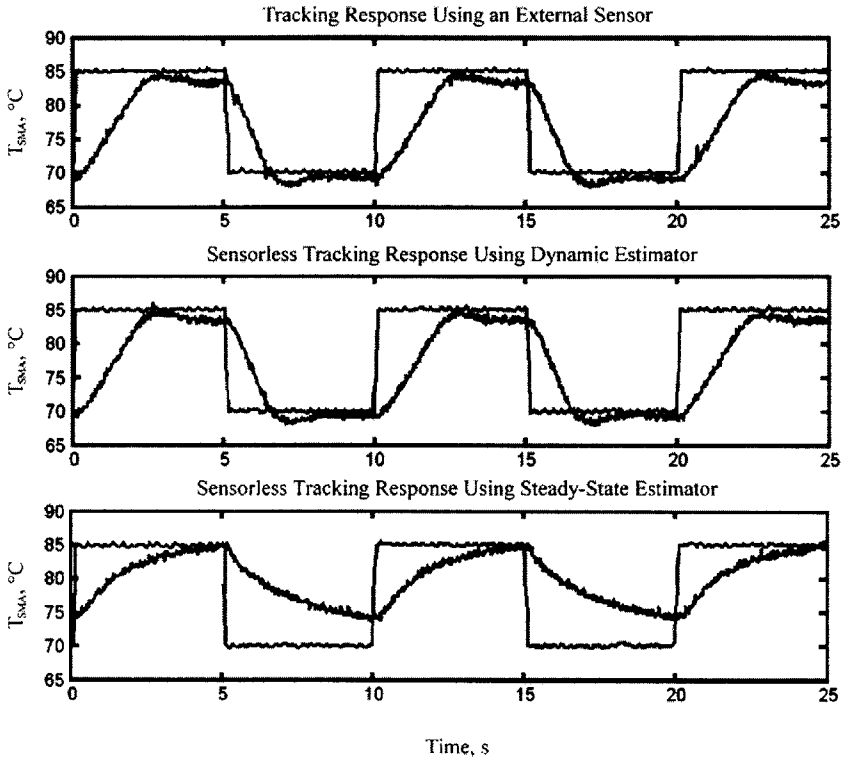

Fig. 7: The use of a dynamic temperature estimator significantly improves the controller's ability to track a time-varying reference signal. The response plotted was measured with an external temperature sensor.

5 Conclusion

Most transduction effects in nature are bi-directional; the thermoelectric devices examined in this thesis are but one example. Piezoelectric crystals are commonly available both as pressure sensors and high-force, low-displacement actuators. Brushless DC motors often use back-induction to measure motor speed. With the advent of ubiquitous, low-cost computing power, the duality of many of these phenomena can be exploited to improve cost and performance through the additional information that can be measured or estimated.

Using the techniques described in this paper, high-DOF TED-driven SMA actuator arrays can be constructed which can be rapidly heated and cooled without external sensors. Because there is no longer a need to occupy TED surface area with temperature sensors, it may be possible to significantly decrease the size of the TEDs behind the individual SMA segments, thereby increasing efficiency and enabling the construction of compact arrays. However, it should be noted that while this technique was developed for the control of shape memory alloy actuators, it should be broadly applicable to any temperature control problem involving thermoelectric devices.

References

[1] Jones, J D; Shahin, A R; Meckl, P H; Thrasher, M A 1994, "Enhanced cooling of shape memory alloy wires using semiconductor "heat pump" modules," J. Intelligent Mater. Syst. Struct. 5, no. 1, pp. 95-104.

[2] Bhattacharyya, A., Lagoudas, D.C., Wang, Y.C., and Kinra, V.K., 1995, "On the Role of Thermoelectric Heat Transfer in the Design of SMA Actuators: Theoretical Modeling and Experiment," Journal of Smart Materials and Structures, 4, pp. 252-263.

[3] Luo, Y., Yakuma, K., Takagi, T., Maruyama, S., 2004, "Thermal responses of a thermoelectric SMA manipulator," International Journal of Applied Electromagnetics and Mechanics, 19, pp. 303-307

[4] Luo, Y., Yakuma, K., Takagi, T., Maruyama, S., 2000, "A Shape Memory Alloy Actuator Using Peltier Modules and R-Phase Transition," Journal of Intelligent Material Systems and Structures 11, pp. 503–511.

[5] Selden, B.; Cho, K. J.; Asada , H. H. , "Segmented binary control of shape memory alloy actuator systems using the peltier effect", Proceedings of the 2004 IEEE International Conference on Robotics and Automation, pp. 4931-4936.

[6] Gray, P., 1960, The Dynamic Behavior of Thermoelectric Devices, M.I.T. Press & John Wiley and Sons, New York.

[7] Lienhard, J. H., Lienhard, J. H., 2005, A Heat Transfer Textbook, 3rd ed., Phlogiston Press, Lexington, MA

[8] Lau, P., Buist, R., 1996, "Temperature and Time Dependent Finite-Element Model of a Thermoelectric Couple," Proceedings of the 15th International Conference on Thermoelectrics, pp. 227-233.